Carbohydrate Polymers 78 (2009) 743–752

Contents lists available at ScienceDirect

Carbohydrate Polymers

journal homepage: www.elsevier.com/locate/carbpol

Methylated *N*-aryl chitosan derivative/DNA complex nanoparticles for gene delivery: Synthesis and structure–activity relationships

Warayuth Sajomsang [a,*], Uracha Ruktanonchai [a], Pattarapond Gonil [a], Varissaporn Mayen [a], Praneet Opanasopit [b]

[a] National Nanotechnology Center, Nanodelivery Laboratory System, National Science and Technology Development Agency, Thailand Science Park, Pathumthani 12120, Thailand
[b] Nanotechnology for Drug/Gene Delivery Systems Group, Department of Pharmaceutical Technology, Faculty of Pharmacy, Silpakorn University, Nakhonpathom 73000, Thailand

ARTICLE INFO

Article history:
Received 13 May 2009
Received in revised form 4 June 2009
Accepted 9 June 2009
Available online 14 June 2009

Keywords:
Chitosan
Methylated *N*-aryl chitosan derivatives
Gene carrier
DNA

ABSTRACT

In this study, three kinds of methylated chitosan containing different aromatic moieties were synthesized by two steps, reductive amination and methylation, respectively. The chemical structures of all methylated derivatives, methylated *N*-(4-*N*,*N*-dimethylaminocinnamyl) chitosan chloride (MDMCMChC), methylated *N*-(4-*N*,*N*-dimethylaminobenzyl) chitosan chloride (MDMBzChC), and methylated *N*-(4-pyridinylmethyl) chitosan chloride (MPyMeChC) were characterized by ATR–FTIR and ^{1}H NMR spectroscopy. The complexes between the chitosan derivatives and plasmid DNA at different N/P ratios were characterized by gel electrophoresis, dynamic light scattering, and atomic force microscopic techniques. The smallest particle sizes of these complexes were obtained at N/P ratio of 5 and ranged from 95 to 124 nm while the zeta-potentials were in the range of 18–27 mV. Transfection efficiencies of these complexes were investigated by expression of the plasmid DNA encoding green fluorescence protein (pEGFP-C2) on human hepatoma cells (Huh 7 cells) compared to *N*,*N*,*N*-trimethyl chitosan chloride (TMChC). The rank of transfection efficiency was MPyMeChC > MDMBzChC > TMChC > MDMCMChC, respectively. The cytotoxicity of these complexes was also studied by MTT assay where the MPyMeChC complex exhibited less toxicity than other derivatives even at high N/P ratios. Therefore, MPyMeChC demonstrated potential as its safe and efficient gene carrier.

1. Introduction

Gene delivery has been regarded as a powerful tool for curing disease by replacing defective genes, substituting missing genes, or silencing unwanted gene expression. There are two approaches of gene delivery: viral and non-viral. Viral delivery is a conventional approach because viruses have evolved to infect cells with high efficacy. However, clinical trials have underscored the safety risks of viral gene delivery due to its possibility to cause cancer and death (Check, 2005; Hollon, 2000). For these reasons, much attention has been focused on non-viral approach according to its potentials to overcome many inherent challenges of viral vectors. Limitations of a viral approach, including small cargo capacity, resistance to repeated infection, difficulty in production and quality control and low safety, can be potentially overcome with a non-viral approach. Physical strategies such as hydrodynamic delivery, electroporation, gene gun, ultrasound, jet injection, magnetofection and photochemical internalization have been used (Wagner, Kircheis, & Walker, 2004). Though these techniques can aid in DNA delivery, there are still problems due to inefficient uptake and poor biostability. Numerous biomaterials have been studied as potential non-viral gene carriers to improve DNA stability and cell uptake such as inorganic surfaces (Kneuer et al., 2000), cationic lipids (Zhang et al., 2004), polysaccharides, cationic polymers, and dendrimers (Merdan, Kopeček, & Kissel, 2002; Putnam 2006; Wong, Pelet, & Putman, 2007). Many polymeric cationic systems such as polyethylenimine (PEI), poly(L-lysines) (PLL), poly(2-(dimethylamino)ethylmethacrylate) (PDMAEMA), and chitosan have been studied for *in vitro* as well as *in vivo* applications (Boussif et al., 1995; Lee, Kwon, Kim, Jo, & Jeong, 1998; Mansouri et al., 2004). Cationic polymers have more advantages than cationic lipids and cationic liposomes due to its high possibility to design various constructions. Moreover, they are able to condense DNA molecules to a relatively small size. This property is very crucial for gene delivery, since small particle size is favorable for improving transfection efficiency (Lv, Zhang, Wang, Cui, & Yan, 2006).

Chitosan (Ch) is a natural cationic polymer consisting of 1–4 linked *N*-acetyl-D-glucosamine (GlcNAc) and D-glucosamine (GlcN) subunits. It is derived from chitin by alkaline hydrolysis which is obtained from the shells of crustaceans, cuticles of insect, and cell wall of fungi and yeasts. Chitosan has attracted significant interest in a broad range of scientific areas such as biomedical, agricultural, and environmental fields because it is non-toxic, biocompatible,

* Corresponding author. Tel.: +66 2 564 7100; fax: +66 2 564 6981.
E-mail address: warayuth@nanotec.or.th (W. Sajomsang).

0144-8617/$ - see front matter © 2009 Elsevier Ltd. All rights reserved.
doi:10.1016/j.carbpol.2009.06.006

and biodegradable in human body. Therefore, it has been proposed as a safer alternative to other non-viral carrier such as cationic lipids and other cationic polymers (Kim et al., 2007; Weecharangsan, Opanasopit, Ngawhirunpat, Rojanarata, & Apirakaramwong, 2006). However, the applications of chitosan are still limited due to its insolubility in water. Moreover, its low specificity and transfection efficiency of chitosan should be overcome for its use in clinical trials (Kim et al., 2007). To improve the water solubility and gene transfection efficiency, the quaternary ammonium Ch derivatives have been previously synthesized (Germershaus, Mao, Sitterberg, Bakowsky, & Kissel, 2008; Kean, Roth, & Thanou, 2005; Murata, Ohya, & Ouchi, 1997). Although, these derivatives were used as alternative for gene carriers, few were successful in increasing transfection efficiency. Many factors for example degree of deacetylation, molecular weight, pH, serum, charge ratio of chitosan to DNA and cell type, can affect on transfection efficiency. However, less attention has been paid on an effect of polymer structures that may influence its physicochemical properties. Therefore, the water-soluble chitosan derivatives, methylated *N*-(4-*N*,*N*-dimethylaminobenzyl) chitosan chloride (MDMBzChC), methylated *N*-(4-pyridinylmethyl) chitosan chloride (MPyMeChC) and methylated *N*-(4-*N*,*N*-dimethylaminocinnamyl) chitosan chloride (MDMCMChC), containing different chain lengths and aromatic moieties were synthesized in this study. To evaluate the role of polymer architecture in gene transfection efficiency, the polymer/DNA ratios on binding affinity, particle size, zeta-potential, morphology, cytotoxicity and transfection efficiency were determined and compared with *N*,*N*,*N*-trimethyl chitosan chloride (TMChC).

2. Experimental

2.1. Materials

Chitosan with molecular weight (M_w) 276 kDa was purchased from Seafresh Chitosan (Lab.) Co. Ltd. (Bangkok, Thailand). The degree of deacetylation (DDA) of chitosan was determined to be 94% by ^{1}H NMR spectroscopy (Lavertu et al., 2003). A dialysis tubing with M_w cut-off of 12,000–14,000 g/mol from Cellu Sep T4, Membrane Filtration Products Inc. (Segiun, TX, USA) was used to purify all modified chitosan derivatives. Polyethylenimine (PEI), M_w 25 kDa, was purchased from Aldrich (Milwaukee, USA). Iodomethane, sodium iodide, and 1-methyl-2-pyrrolidone (NMP) were purchased from Acros Oganics (Geel, Belgium). 4-Dimethylaminobenzaldehyde, 4-dimethylaminocinnamaldehyde, 4-pyridinecarboxaldehyde and sodium cyanoborohydride ($NaCNBH_3$) were purchased from Fluka (Deisenhofen, Germany). 3-(4,5-Dimethylthiazol-2-yl)-2, 5-diphenyl tetrazolium bromide (MTT) was purchased from Sigma-Chemical Co. (St. Louis, MO, USA). Dulbecco's modified Eagle's medium (DMEM), Trypsin–EDTA, penicillin–streptomycin antibiotics, and fetal bovine serum (FBS) were obtained from GIBCO-Invitrogen (Grand Island, NY, USA). The human hepatocellular carcinoma (Huh 7) cell lines were obtained from the American Type Culture Collection (ATCC, Rockville, MD, USA). All other chemicals were of cell culture and molecular biology grade.

2.2. Synthesis of N-aryl chitosan derivatives

N-(4-*N*,*N*-dimethylaminocinnamyl) chitosan (DMCMCh) were prepared according to the previously reported procedure (Scheme 1) (Sajomsang, Tantayanon, Tangpasuthadol, & Daly, 2008). In brief, 1.0 g of Ch was dissolved in 70 mL of 1% (v/v) acetic acid. The solution was diluted with ethanol 70 mL, and then 1.07 g of 4-dimethylaminocinnamaldehyde was added to the solution. The reaction mixture was stirred at 60 °C for 12 h. At this point the pH of the solution was adjusted to 5 by adding 15% (w/v) NaOH. Then, 1.54 g of $NaCNBH_3$ was added, and the resulting solution was allowed to stir at room temperature for 24 h, followed by adjusting the pH to 7 with 15% (w/v) NaOH. The aqueous solution was dialyzed against de-ionized (DI) water for 3 days, followed by freeze drying (1.33 g, 86.0% yield, and DS = 76%). Using the same technique described above, the designated aromatic aldehydes, 4-dimethylaminobenzaldehyde and 4-pyridinecarboxaldehyde were used instead of 4-dimethylaminocinnamaldehyde.

DMCMCh. ATR–FTIR; ν 3384 (O—H and N—H, GlcN), 2912, 2847, and 2798 (C—H, GlcN), 1611 and 1518 (C=C, Aromatic), 1131 (C—O—C, GlcN), 1056 and 1021 cm^{-1} (C—O, GlcN), 801 cm^{-1} (C—H, Aromatic). ^{1}H NMR (CD_3COOD): δ (ppm) 7.5 (m, 4H, Ph), 4.8 (s, 1H, H1), 4.5 (d, 2H, CH_2-NH), 4.5–3.0 (m, 6H, H2-H6) 3.1 (s, 6H N(CH_3)$_2$), 3.0 (s, 1H H2), 1.9 (s, 3H, NHAc).

DMBzCh. ATR–FTIR; ν 3384, 1615, 1520, 1147, 1054, 1021, and 799 cm^{-1}. ^{1}H NMR (D_2O/CF_3COOD): δ (ppm) 7.5 (s; 4H Ph), 4.9 (s; 1H H1), 4.4 (s, 2H, CH_2-NH), 4.4–3.3 (m, 5H, H2-H5), 3.1 (s; 6H N(CH_3)$_2$ Ph), 2.9 (br. s; 1H H2), 1.9 (s; 3H NHAc).

PyMeCh. ATR–FTIR; ν 3292, 1605, 1556, 1419, 1149, 1064, 1026, and 797 cm^{-1}. ^{1}H NMR (D_2O/CF_3COOD): δ (ppm) 7.2–6.9 (dd; 4H Py), 4.4 (br. m; 2H CH_2-NH) 4.4–3.0 (m, 5H H2-H3), 3.0 (br. s; 1H H2), 1.91 (s; 3H NHAc).

2.3. Synthesis of N,N,N-trimethyl chitosan chloride (TMChC)

Chitosan was methylated with iodomethane yielded TMChC in accordance to a reported procedure (Scheme 2) (Elisabete, Douglas, & Sergio, 2003; Sajomsang et al., 2008). In brief, 1.0 g of Ch was dispersed in 50 mL of 1-methyl-2-pyrrolidone (NMP) at room temperature and the mixture was stirred for 12 h. Then 8 mL of 15% (w/v) NaOH was dropped slowly in the solution. Sodium iodide (3.0 g) was added and the mixture was stirred at 60 °C for 15 min. Subsequently, 3, 3, and 2 mL of iodomethane was added three times, respectively every 4 h and the mixture was stirred at 60 °C for 24 h. After methylation, TMChC was precipitated in 300 mL of acetone. The precipitate was filtered and dissolved in 50 mL of NMP. The TMChC was further methylated by using the same procedure as described above. The precipitate was dissolved in 15% (w/v) NaCl in order to replace the iodide counter-ion with a chloride counter-ion. The suspension was dialyzed with DI water for 3 days to remove inorganic materials and then freeze-dried.

TMChC. ATR–FTIR; ν 3304 (O—H and N—H, GlcN), 1473 (C—H, N$^+$(CH_3)$_3$), 1144, (C—O—C, GlcN), 1047, and 1029 cm^{-1} (C—O, GlcN). ^{1}H NMR (D_2O): δ (ppm) 5.4 (br. s; 1H H1′), 4.4–3.0 (br. m; 22H H2-H6, s; 6H 3, 6-*O*-CH_3; s, 9H N$^+$(CH_3)$_3$), 2.7 (br. m; 6H N(CH_3)$_2$), 2.3 (s; 3H NHCH_3), 1.9 (s; 3H NHAc). ^{13}C NMR (D_2O): δ (ppm) 96.5 (C1), 77.6 (C4), 74.7 (C5), 68.8 (C5), 60.0–55. (C2 and C6), 54.4 (N$^+$(CH_3)$_3$), 42.7 (N(CH_3)$_2$).

2.4. Methylation of N-aryl chitosan derivatives

The *N*-aryl chitosan derivatives were methylated by a single treatment with iodomethane yielded methylated *N*-aryl chitosan derivatives as the same procedure described above (Scheme 2).

MDMCMChC. ATR–FTIR; ν 3357, (O—H and N—H, GlcN), 1658, 1510 (C=C, Aromatic), 1465 (C—H, N$^+$(CH_3)$_3$), 1107 (C—O—C, GlcN), 1046 and 1013 cm^{-1} (C—O, GlcN), 847 cm^{-1} (C—H, Aromatic). ^{1}H NMR (D_2O): δ (ppm) 7.9–7.3 (m, 4H, Ph), 6.7–6.3 (dd, 2H C*H* = C*H*), 5.1 (br. s; 1H H1′), 4.6–3.0 (33H, m, 7H CH_2-NH and H2-H6; s, 9H N$^+$(CH_3)$_3$ Ph; s, 6H 3, 6-*O*-C H_3; s, 9H N$^+$(CH_3)$_3$), 2.7 (s, 6H N(CH_3)$_2$), 1.9 (s, 3H, NHAc).

MDMBzChC. ATR–FTIR; ν 3380, 1660, 1506, 1467, 1098, 1044, 1017, and 872 cm^{-1}. ^{1}H NMR (D_2O): δ (ppm) 7.8–7.5 (dd; 4H Ph), 5.1 (br. s; 1H H1′), 4.6–3.0 (33H, m, 7H CH_2-NH and H2-H6; s, 9H

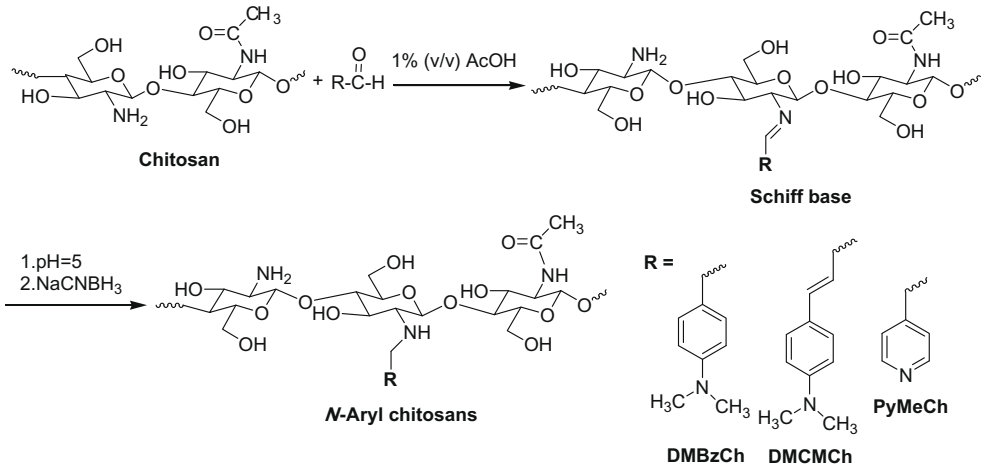

Scheme 1. Synthesis of *N*-aryl chitosan derivatives.

$N^+(CH_3)_3$ Ph; s, 6H 3, 6-*O*-CH_3; s, 9H $N^+(CH_3)_3$), 2.7 (s, 6H $N(CH_3)_2$), 1.9 (s; 3H NHAc). ^{13}C NMR (D_2O): δ (ppm) 145.5, 141.5, 130.9, 119.5 (C-Ph), 96.5 (C1), 77.1–58.6 (C2, C3, C4, C5, and C6), 56.9 ($N^+(CH_3)_3$ Ph), 53.8 ($N^+(CH_3)_3$), 41.7 ($N(CH_3)_2$), 36.3 ($NHCH_3$).

MPyMeChC. ATR–FTIR; ν 3347, 1570, 1469, 1192, 1098, 1040, and 845 cm^{-1}. ^{1}H NMR (D_2O): δ (ppm) 8.6–7.9 (dd; 4H Py), 5.1 (br. s; 1H H1′), 4.6–3.0 (br. m; 26H CH_2-NH, H2-H6, s, 6H 3, 6-*O*-CH_3, s; N^+CH_3 Py, s; 9H $N^+(CH_3)_3$), 2.5 (s; 6H $N(CH_3)_2$), 1.9 (s; 3H NHAc). ^{13}C NMR (D_2O): δ (ppm) 174.9, 160.6, 144.8, 127.4 (C-Py), 96.55 (C1), 78.8–60.9 (C2, C3, C4, C5, and C6), 68.3 (N^+CH_3 Py), 54.4 ($N^+(CH_3)_3$), 42.7 ($N(CH_3)_2$).

2.5. FTIR and ^{1}H NMR spectroscopy

The solid samples of chitosan derivatives were characterized by using the single bounce ATR–FTIR spectroscopy (Smart Orbit accessory) with a diamond internal reflection element (IRE). All ATR–FTIR spectra were performed with the Nicolet 6700 spectrometer (Thermo company, USA) at the ambient temperature (25 °C) by using standard spectral collection techniques and the rapid-scan software in OMNIC 7.0. In all cases, the spectra were collected using 32 scans with a resolution of 4 cm^{-1}. The ^{1}H and ^{13}C NMR spectra were measured on a Bruker AVANCE 500 MHz spectrometer. All measurements were performed at 300 K and 1% (v/v) of D_2O/CF_3COOD and D_2O were used as solvents for chitosan and its methylated derivatives, respectively.

2.6. Determination of molecular weight of chitosan and its methylated derivatives

The weight average molecular weight (M_w), number average molecular weight (M_n), and M_w/M_n of chitosan and its derivatives were determined using a gel permeation chromatography (GPC). It consists of Waters 600E Series generic pump, injector, ultrahydrogel linear columns (M_w resolving range 1–20,000 kDa), guard column, pollulans as standard (M_w 5.9–788 kDa), and refractive in-

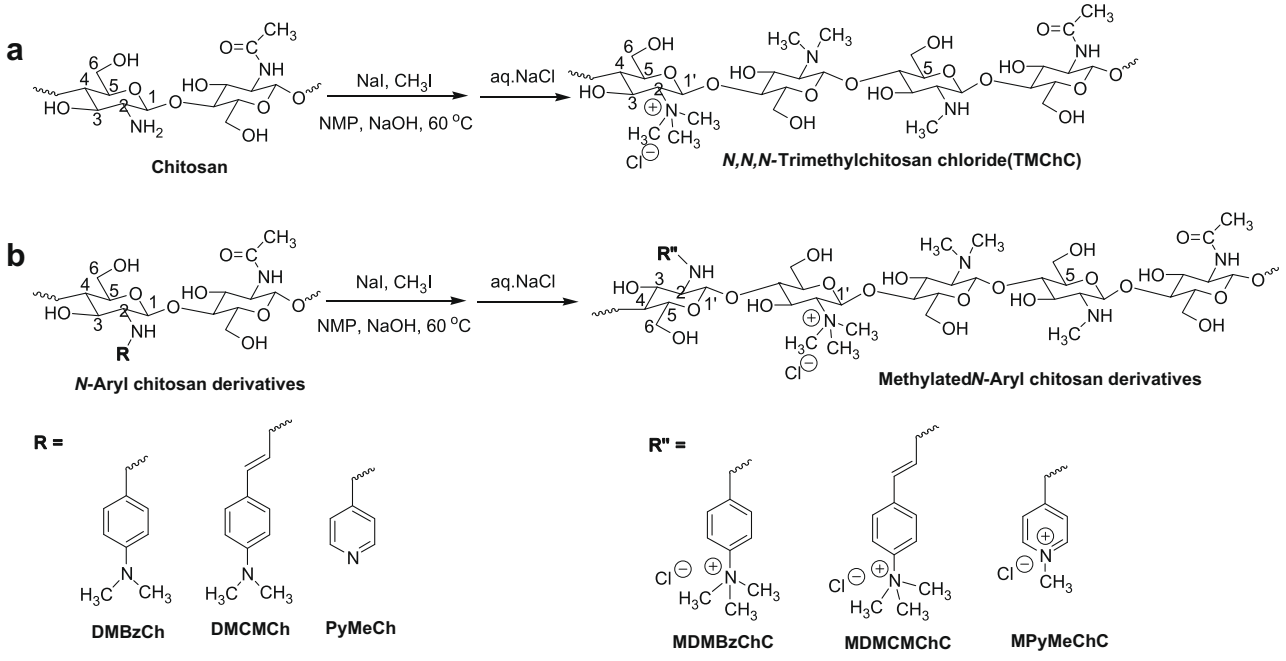

Scheme 2. Synthesis of methylated chitosan derivatives (a) *N*,*N*,*N*-trimethyl chitosan chloride (TMChC) and (b) methylated *N*-aryl chitosan derivatives.

dex detector (RI). All samples were dissolved in acetate buffer pH 4 and then filtered through VertiPure nylon syringes filters 0.45 μm (VERTIC Vertical chromatography Co. Ltd., Thailand). The mobile phase was 0.5 M AcOH and 0.5 M AcONa (acetate buffer pH 4) at a flow rate of 0.6 mL/min at 30 °C and the injection volume 20 μL was used.

2.7. Estimation of water solubility

The water solubility of methylated *N*-aryl chitosan derivatives and TMChC with various pHs was estimated using turbidity measurements. The sample was dissolved in de-ionized water. Then 0.1 or 1 M HCl solution and 0.1 or 1.0 M NaOH solution were added. The transmittance of the solution was recorded on a Lamda 650 UV/VIS Spectrophotometer (Perkin-Elmer, USA) with an optical path length of 350 nm at 600 nm. The test was performed at 25 °C.

2.8. Plasmid DNA preparation and bacterial culture

The plasmid DNA used in this study was pEGFP-C2 (Clontech, Palo Alto, USA) encoding green fluorescent protein (GFP), which originally cloned from the mutant *Aequorea victoria*. The pEGFP-C2 was amplified in *Escherichia coli* DH101 strain, which was cultured in Luria–Bertani (LB) broth {1% (w/v) tryptone, 0.5% (w/v) yeast extract (Difco, USA), 0.5% (w/v) NaCl (Molekula, UK)} containing 0.015 mg/mL kanamycin (GIBCO, USA) then grown at 37 °C with shaking at 250 rpm. The pEGFP-C2 was extracted using QIAGEN Hispeed plasmid midi kits (Qiagen, Germany). The size and concentration of DNA was examined by comparing with the Mass Ruler DNA ladder mix (Fermentas, USA) on 1% agarose gel electrophoresis in Tris–boric acid–EDTA (TBE) buffer (BioRad, USA) and concentration was confirmed by absorbance measurement at 260 and 280 nm using SpectraMax M2 microplate readers (MDS Inc., Toronto, Canada).

2.9. Gel retardation assay

To determine the binding capacity of Ch derivatives with pEGFP-C2, the N/P ratios of methylated Ch derivatives to pEGFP-C2 were varied from 0.5 to 4. The mixture (10 μL) containing DI water, pEGFP-C2 (1 μg) and Ch derivatives were mixed and then allowed to form complexes at 25 °C for 15 min. The methylated Ch derivatives/pEGFP-C2 complexes were loaded in each well and the electrophoresis was carried out at 100 V for 40 min. The samples were analyzed under UV transilluminator (Syngene, UK) after staining with 1 μg/mL of ethidium bromide.

2.10. Dynamic light scattering and zeta-potential measurements

The *Z*-average hydrodynamic diameter, polydispersity index (PDI), and surface charge of methylated Ch derivatives/DNA complexes were determined by dynamic light scattering (DLS) using Zetasizer Nano ZS (Malvern Instruments Ltd., Malvern, UK) at 25 °C. The complexes were prepared at varying N/P ratios and diluted with DI water. All samples were measured in triplicate.

2.11. Atomic force microscopy (AFM)

Morphology of the polyplexes was determined by atomic force microscopy (AFM) using dynamic force microscope (DFM) mode (Seiko, Japan). The complexes at N/P ratios of 5 were prepared and incubated for 15 min. The mixture (5 μL) was then subjected to freshly cleaved mica and dried at room temperature. All images were obtained with a scan rate of 0.5 Hz over a selected area of 5 × 5 μm, 2 × 2 μm and 1 × 1 μm.

2.12. Cytotoxicity assay

The evaluation of cytotoxicity was performed by the MTT assay. Huh 7 cells were seeded in a 96-well plate at a density of 5×10^4 cells/cm^2 in 200 μL of growth medium and incubated for 24 h at 37 °C under 5% CO_2 atmosphere. Prior to transfection, the medium was removed and the cells were rinsed with PBS, and then supplied with the methylated Ch derivatives/DNA complexes at the same concentrations as *in vitro* transfection experiment. After treatment, methylated Ch derivatives/DNA complexes solutions were removed. Finally, the cells were incubated with 100 μL MTT containing medium (1 mg/mL) for 4 h. Then the medium was removed, the cells were rinsed with PBS, pH 7.4, and formazan crystals formed in living cells were dissolved in 100 μL DMSO per well. Relative viability (%) was calculated based on absorbance at 550 nm using a microplate reader (Universal Microplate Analyzer, Model AOPUS01 and AI53601, Packard BioScience, CT, USA). Viability of non-treated control cells was arbitrarily defined as 100%.

2.13. In vitro transfection

Transfection studies were performed in Huh 7 cells using the pEGFP-C2 as a marker gene. Huh 7 cells were seeded for 24 h into 24-well plates at a density of 5×10^4 cells/cm^2 in 1 mL of growth medium (DMEM containing 10% FBS, supplemented with 2 mM L-glutamine, 1% non-essential amino acid solution, 100 U/mL penicillin and 100 μg/mL streptomycin). The cells were grown under humidified atmosphere (5% CO_2, 37 °C) for 24 h. Prior to transfection, the medium was removed and the cells were rinsed with phosphate-buffered saline (PBS, pH 7.4). The cells were incubated with 0.5 mL of the methylated Ch derivatives/DNA complexes at various N/P ratios containing 1 μg of DNA for 24 h at 37 °C under 5% CO_2 atmosphere. Non-treated cells and cells transfected with naked plasmid and PEI/DNA complexes were used as controls. After transfection, the cells were washed with PBS twice and grown in culture medium for 48 h to allow GFP expression. All transfection experiments were performed in triplicate.

2.14. Statistical analysis

Statistical significance of differences in transfection efficiency and cell viability were examined using one-way analysis of variance (ANOVA) followed by an LSD *post hoc* test. The significance level was set at $p < 0.05$.

3. Results

3.1. Synthesis and characterization of methylated chitosan derivatives

Following the synthesis route shown in Scheme 1, *N*-aryl chitosan derivatives were successfully obtained by reductive amination of the corresponding Schiff base intermediates. It is a versatile and specific method for creating a covalent bond between a substrate and the amine function of the Ch. The degree of *N*-substitution (DS) was determined by ^{1}H NMR spectroscopic method (Crini et al., 1997). It was found that the DS were in the range of 70–75%. Table 1 summarized the results of chitosan with various aromatic aldehydes. Methylation of *N*-aryl chitosan derivatives was carried out by single treatment with iodomethane which yielded the corresponding quaternary ammonium chitosan derivatives. The methylation was occurred at both the aromatic substituent and the primary amino groups of Ch (Sajomsang et al., 2008) and the degree of quaternization (DQ) was shown in Table 2. It was found that the DQ was in the range of 78–82% which was

Table 1
N-arylation of chitosan with various aromatic aldehydes.

Samples	Molar ratio (aldehyde:GlcN)	Targeted DS (%)	FW	Obtained DS	Yield (%)
DMBzCh	3:1	300	249.48	70	88.6
DMCMCh	2:1	200	284.36	76	70.0
PyMeCh	2:1	200	225.40	68	76.7

FW is the formula weight of repeating unit = 12.2 + (FW of *N*-aryl GlcN × DS) + [161 × (0.94-DS)].
DS is the degree of *N*-substitution.
Yield (%) = (Weight of *N*-aryl chitosan (g) × [163.5/weight of chitosan (g) × theoretical calculated FW of *N*-aryl GlcN)] × 100.

Table 2
Methylation of chitosan and *N*-aryl chitosan derivatives.

Samples	DS (%)	DQ_T (%)		$N(CH_3)_2$ (%)	$NHCH_3$ (%)	Total *O*-CH_3 (%)	Recovery (%)
		DQ_{Ar} (%)	DQ_{Ch} (%)				
TMChC	–	–	65	25	5	35	74
MDMBzChC	70	70	8	10	–	18	120
MDMCMChC	76	76	6	10	–	26	109
MPyMeChC	68	68	12	8	Trace	20	60

DQ_{Ar} is the degree of quaternization at aromatic substituents, DQ_{Ch} is the degree of quaternization, $N(CH_3)_2$ is the *N,N*-dimethylation , $NHCH_3$ is the *N*-methylation. Total *O*-CH_3 is the total degree of *O*-methylation of 3-*O* and 6-*O* at 3-hydroxyl and 6-hydroxyl positions of GlcN of chitosan, respectively. Recovery (%) is [weight of methylated product (g)/weight of *N*-aryl chitosan (g)] × 100.

calculated by ^{1}H NMR spectroscopy (Sieval et al., 1998). Besides quaternization, *N,N*-dimethylation, *N*-methylation, and *O*-methylation at the primary amino groups and hydroxyl groups of Ch were also observed.

The chemical structures of Ch and its derivatives were characterized by ATR–FTIR and ^{1}H NMR spectroscopy. Fig. 1 exhibited the ATR–FTIR pattern of Ch. The absorption bands at wave numbers 3357 cm^{-1} were due to OH and NH_2 groups, whereas those at 1639 and 1374 cm^{-1} were corresponded to the C═O and C—O stretching of amide group. The band at 1583 cm^{-1} was due to N—H deformation of amino groups, and the bands at 1147, 1056 and 1026 cm^{-1} were corresponded to the symmetric stretching of the C—O—C and involved skeletal vibration of the C—O stretching (Brugnerotto et al., 2001). The ATR–FTIR spectra of MDMBzChC, MDMCMChC, and MPyMeChC showed the additional absorption bands at wavenumbers around 1611, 1518, and 801 cm^{-1}, respectively. These bands were assigned to the C═C stretching and C—H deformation (out of plane) of the aromatic group. Besides, all methylated Ch derivatives exhibited the characteristic ATR–FTIR spectrum at wavenumbers in the range of 1465–1473 cm^{-1}, which were due to C—H symmetric bending of the methyl substituent of quaternary ammonium groups (Kim, Choi, Chun, & Choi, 1997). Fig. 2 exhibited ^{1}H NMR spectra of MDMCMChC, MDMBzChC, and MPyMeChC. The proton signal at δ 3.5 ppm was assigned to the *N,N,N*-trimethyl protons of cinnamyl or benzyl substituent while the proton signals at δ 3.2, 2.7 and 2.3 were assigned to *N,N,N*-trimethyl protons, *N,N*-dimethyl protons and *N*-methyl protons of GlcN, respectively. Furthermore, *O*-methylation was also observed at δ 3.3 and 3.4 ppm which were assigned to 6-*O*-methylated and 3-*O*-methylated protons.

3.2. Molecular weight determination

The weight average molecular weight (M_w), the number average molecular weight (M_n) and the M_w/M_n of chitosan and its derivatives were determined by gel permeation chromatography (GPC), which is presented in Table 3. The M_n, M_w and M_w/M_n of molecular

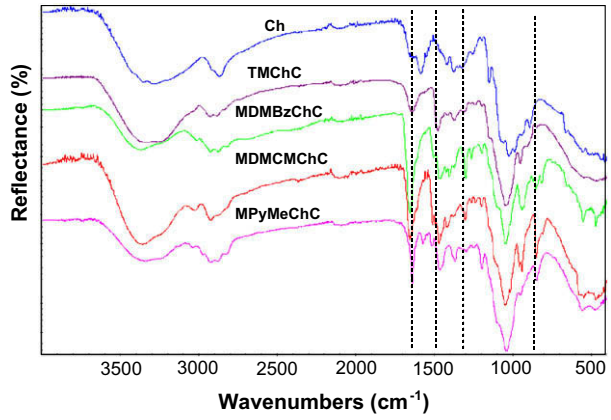

Fig. 1. ATR–FTIR spectra of chitosan (Ch), *N,N,N*-trimethyl chitosan chloride (TMChC), methylated *N*-(4-*N,N*-dimethylaminobenzyl) chitosan chloride (MDMBzChC), methylated *N*-(4-*N,N*-dimethylaminocinnamyl) chitosan chloride (MDMDMChC), and methylated *N*-(4-pyridinylmethyl) chitosan chloride (MPyMeChC).

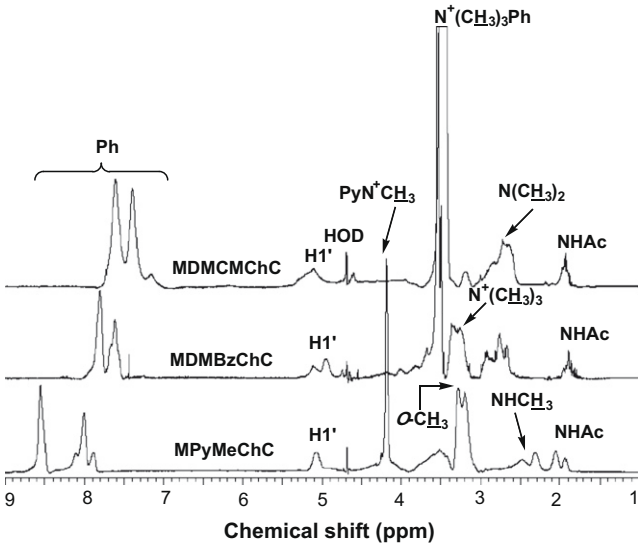

Fig. 2. ^{1}H NMR spectra of methylated *N*-(4-*N,N*-dimethylaminobenzyl) chitosan chloride (MDMBzChC), methylated *N*-(4-*N,N*-dimethylaminocinnamyl) chitosan chloride (MDMDMChC), and methylated *N*-(4-pyridinylmethyl) chitosan chloride (MPyMeChC) in D_2O.

Table 3
Weight average molecular weight (M_w), number average molecular weight (M_n), and M_w/M_n of chitosan before and after methylation.

Samples	DS (%)	DQ_T (%)	M_n (kDa)	M_w (kDa)	M_w/M_n
Chitosan	–	–	48.71	276.06	5.67
TMChC	–	65	22.88	120.87	5.28
MDMBzChC	70	78	9.99	70.09	7.01
MDMCMChC	76	82	26.23	40.35	1.53
MPyMeChC	68	80	6.16	12.22	1.98

weight average of the native Ch were found as 48.71 kDa, 276.06 and M_w/M_n 5.67, respectively. It was found that a relatively wide molecular weight distribution with a polydispersity index (PDI) of Ch was observed, which was similarly observed in case of TMChC. Moreover, it was found that the methylation reaction led to a significant reduction in the Ch molecular weight. Snyman, Hamman, & Kotze (2003) found that the decreasing in molecular weight of Ch depended on the methylation procedure and more pronounced effect could be found with the extension of reaction duration, corresponding to an increase in DQ. Similar result has been previously report by our research group (Sajomsang et al., 2008). We found that the molecular weight of Ch in the *N*-arylation step decreased slightly. The methylation step leading to methylated Ch derivatives were accompanied by a significant decrease of molecular weight. It was plausible that an oxidative degradation process and alkaline depolymerization would occur.

3.3. Water solubility

Fig. 3 exhibited the pH dependence of the transmittance of the TMChC and methylated *N*-aryl Ch derivatives. It was found that water solubility of MPyMeChC was higher than that of the MDMCMChC and MDMBzChC at all observed pH range. However, its solubility in water similar to TMChC. It should be noted that an introduction of the *N,N*-dimethylaminocinnamyl and *N,N*-dimethylbenzyl groups resulted decrease in a solubility. It was postulated that highly hydrophobicity and steric hindrance of the *N,N*-dimethylaminocinnamyl and *N,N*-dimethylaminobenzyl moiety in the chitosan backbone decreased the water solubility.

3.4. Physicochemical characterization of methylated chitosan derivatives/DNA complexes

The influence of N/P ratios of methylated Ch derivatives and DNA condensation was investigated by agarose gel electrophoresis (Fig. 4). Free naked DNA was shown on Lane 2 while the methylated Ch derivatives/DNA complexes at N/P ratios between 0.5 and 4 were shown in Lanes 3–10. The electrophoretic mobility of DNA was retarded with increasing N/P ratios of the methylated Ch derivatives. The entire DNA band can be retained in the loading well, suggesting complete DNA complex formation with the methylated Ch derivatives. DNA complex formation of TMChC was found at N/P ratio of 3 (Fig. 4a) whereas MPyMeChC MDMBzChC, and MDMCMChC were found at 2.5, 2.5 and 2, respectively (Fig. 4b–d). It is important to note that the complex formation found at different N/P ratios depended on the DQ of derivatives. These results clearly showed that the derivatives at lower DQ could form complete complex formation at higher N/P ratio. This is due to higher charge density of the methylated Ch derivatives required to neutralize DNA phosphate group compared to those of higher DQ.

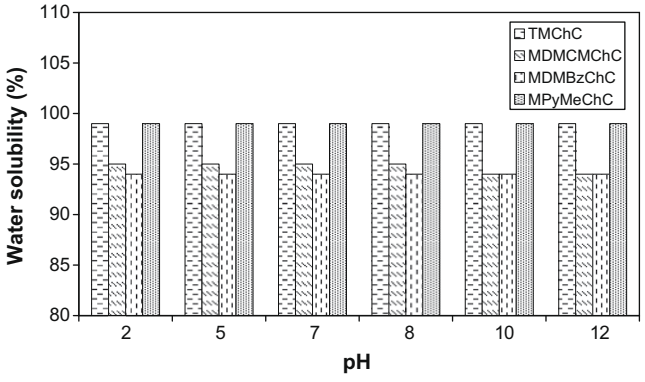

Fig. 3. The pH dependence of water solubility of *N,N,N*-trimethyl chitosan chloride (TMChC) and methylated *N*-aryl chitosan derivatives at 1 mg/mL.

The particle sizes and zeta-potential of formed complexes at pH 7.4 were investigated at various N/P ratios (Fig. 5). The particle sizes of these complexes were in the range of 100–600 nm. The particle sizes of all complexes tended to decrease with an increase in N/P ratios from 0.5 to 5. The smallest particle sizes of these complexes ranged from 95 to 124 nm were all obtained at N/P ratio 5. The size of these complexes at this ratio can be ranked as MDMCMChC > MPyMeChC > TMChC > MDMBzChC, respectively. At higher N/P ratio 10, an increase in complex size was found, which might be due to an aggregation of neutralized complexes (Fig. 5a–d). The zeta-potential of all complexes ranged from −43 to 46 mV were obtained (Fig. 5a–d). At N/P ratios of 0.5–1, negative zeta-potentials were observed, which was due to incomplete condensation between DNA and the methylated Ch derivatives. On the other hand, the positive zeta-potentials were obtained after N/P ratio of 1. This is due to the highly negative charge of DNA, which was rapidly neutralized and the surface charge of the complexes turned into positive values at higher N/P ratios. The zeta-potential is known to be one of the major factors which affected biodistribution and transfection efficiency (Nomura et al., 1997). A presence of positive surface charge would allow an electrostatic interaction to occur between negatively charged cellular membranes and positively charged complexes (Mansouri et al., 2006). In the present study, the smallest complexes ranged from 95 to 124 nm and the zeta-potential ranged from 18 to 27 mV were obtained at N/P ratio of 5.

The methylated Ch derivatives/DNA complexes were characterized by AFM according to N/P ratios from gel retardation assay (Fig. 6). The AFM image revealed that spherical particles and some aggregation were observed in TMChC/DNA complex at N/P ratio of 3 (Fig. 6a). Similar AFM images were found in MDMBzChC/DNA and MDMCMChC/DNA complexes (Fig. 6c and d) with N/P ratios of 2.5 and 2, respectively. The AFM image of MPyMeChC/DNA complex at N/P ratio of 2.5 also demonstrated spherical nanoparticles (Fig. 6b). This may indicate that this complex had DNA folding inside like globular shape in which the MPyMeChC was surrounded around the particles. However, MPyMeChC/DNA complex was aggregated at this N/P ratio. Previously, several reports showed that the spherical structure was observed in the PEI/DNA complex (Köping-Höggård et al., 2001). The short rod- and toroid-like structures were found with cationic polymers complexed with DNA such as poly(amidoamine)s (Martin et al., 2000), polylysine (Golan, Pietrasanta, Hsieh, & Hansma, 1999), and protamine (Allen, Bradbury, & Balhorn, 1997).

3.5. In vitro transfection of methylated chitosan derivatives/DNA complexes

In vitro transfection was performed on human hepatoma cell lines (Huh 7 cells) to investigate gene transfection efficiencies of methylated Ch derivatives (Fig. 7). The pEGFP-C2 plasmid encoding green fluorescent protein (GFP) was used as DNA representative. The complexes were formulated with various N/P ratios in order

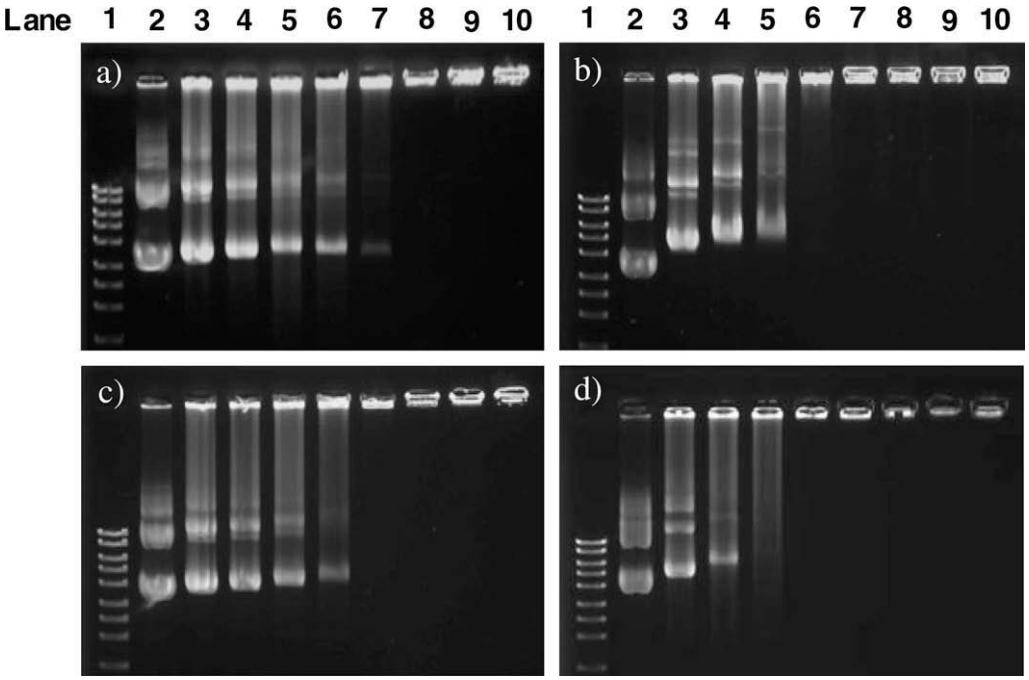

Fig. 4. Gel retardation of methylated chitosan derivatives/plasmid DNA complexes performed with (a) *N*,*N*,*N*-trimethyl chitosan chloride (TMChC), (b) methylated *N*-(4-pyridinylmethyl) chitosan chloride (MPyMeChC), (c) methylated *N*-(4-*N*,*N*-dimethylaminobenzyl) chitosan chloride (MDMBzChC), and (d) methylated *N*-(4-*N*,*N*-dimethylaminocinnamyl) chitosan chloride (MDMDMChC). Lane 1, DNA marker; lane 2, DNA; lanes 3–10, polymers/DNA complexes at N/P ratios of 0.5, 1, 1.5, 2, 2.5, 3, 3.5, and 4, respectively.

to determine the appropriate conditions for gene transfection efficiency. Polyethylenimine (PEI 25 kDa) complexed with DNA at the weight ratio of 1 was used as a positive control. In all studies, no transfection was found in control (cells without complexes) and naked DNA. The highest gene transfection efficiencies of all complexes were observed at N/P ratios 5 due to the smallest particle size (95–124 nm). The transfection efficiencies of all methylated Ch derivatives/DNA complexes on Huh 7 cell can be ranked as MPyMeChC > MDMBzChC > TMChC > MDMCMChC. The transfection efficiencies of all complexes were dramatically decreased when N/P ratios higher than 5. This could possibly due to an increase in cytotoxicity towards Huh 7 cells (Fig. 8). Among four carriers, MPyMeChC demonstrated the highest transfection efficiency with the highest cell viability. It is important to note that the particle sizes and the zeta-potentials of each methylated Ch derivative/DNA complex were not significantly different, therefore other parameters such as polymer structure might play an important role a gene transfection efficiencies.

3.6. Cytotoxicity of methylated chitosan derivatives/DNA complexes

The cationic polymer vectors that used for gene delivery should be safe, therefore, the toxicity of Ch derivatives was investigated. It has been reported that Ch and its derivatives were less toxic than other cationic polymers, such as polylysine and polyethylenimine, both *in vitro* and *in vivo* (Thanou, Florea, Geldof, Junginger, & Borchard, 2002). Various Ch and Ch derivatives had demonstrated their potential roles as new carriers for gene delivery, although their toxicity of those chitosans were varied depending on the type of cells and Ch derivatives. Fig. 8 showed the effect of methylated Ch derivatives/DNA complexes on cell viability. The Huh 7 cells were incubated with only DNA showed the cell viability almost the same as non-transfected cells. At the lowest N/P ratio, the cell viability of the methylated Ch derivatives/DNA complexes was in the range of 80–100% which their sequences were as follow TMChC > MDMCMChC > MPyMeChC > MDMBzChC. It was noted that the cell viability decreased significantly with increasing N/P ratios of the complexes, suggesting an effect of high density of quaternary ammonium moieties on cell viability. However, 70–80% cells viabilities were found at all N/P ratios of MPyMeChC/DNA complex, which indicated that the MPyMeChC/DNA complex was rather safe on Huh 7.

4. Discussion

Several reports showed similar results of such size dependence on gene transfection efficiency (Guy, Drabek, & Antoniou, 1995; Ogris, Steinlein, Carotta, Brunner, & Wagner, 2001; Ogris et al., 1998; Anderson, Akinc, Hossain, & Langer, 2005). Since most polycationics/DNA nanoparticles could be uptake into cell by endocytosis pathway, which is limited to particles size less than 150 nm in diameter (Guy et al., 1995; Anderson et al., 2005). Conflicts still arise on either small or large particles will exhibit better transfection (Ogris et al., 1998, 2001). This demonstrates leads to hypothesis that apart from particle size, other biophysical parameters such as polymer structure, polymer molecular weight and charge ratio may play an important role on transfection efficiency.

Hydrophobic moieties in non-viral carriers are expected to increase transfection efficiency. Since there groups may assist dissociation of polymer/DNA complexes and release facilely of DNA from polymer into cytoplasm. It has been reported that hydrophobic modifications of cationic polymer, lipid and chitosan could assist better transfection capability as an optimal substitution (Chae, Son, Lee, Jang, & Nah, 2005; Doody, Korley, Dang, Zawaneh, & Putnam, 2006). This is expected due to increasing cell membrane/carrier interactions or the destabilization of the cell membranes, easier DNA unpacking from carriers and increasing of entry into cells, facilitation of endocytic uptake, and increasing of escape of complexes from endosome (Chae et al., 2005; Doody et al., 2006; Tian et al., 2007). In the present study, the introduction

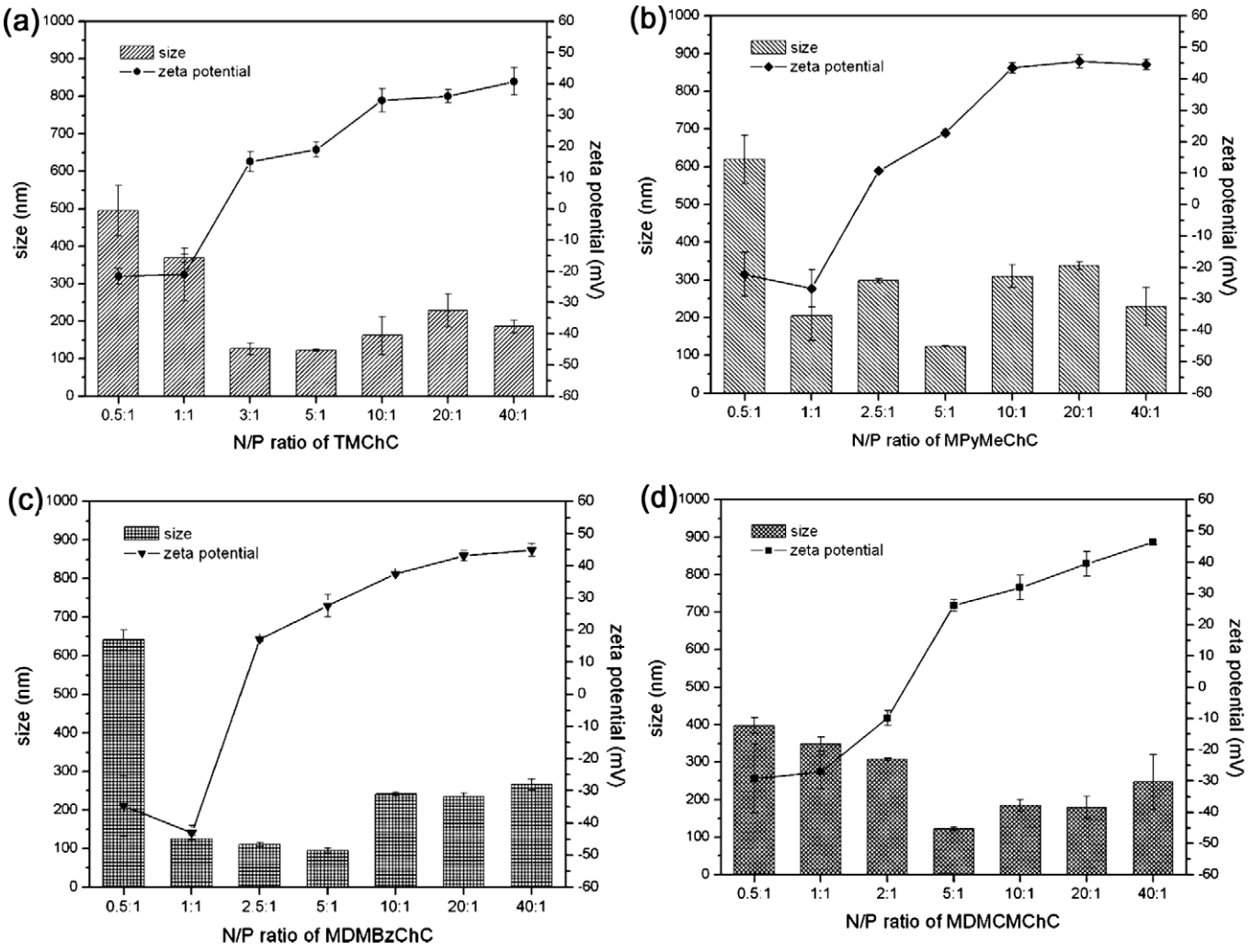

Fig. 5. The size and zeta-potential of methylated chitosan derivatives/pEGFP-C2 complexes formulated with *N,N,N*-trimethyl chitosan chloride (TMChC), (b) methylated *N*-(4-pyridinylmethyl) chitosan chloride (MPyMeChC), (c) methylated *N*-(4-*N,N*-dimethylaminobenzyl) chitosan chloride (MDMBzChC), and (d) methylated *N*-(4-*N,N*-dimethylaminocinnamyl) chitosan chloride (MDMDMChC) at N/P ratios 0.5–40.

of *N,N*-dimethylaminocinnamyl and *N,N*-dimethylaminobenzyl moieties into the Ch backbone was expected to enhance the hydrophobicity of the carriers. However, their transfection efficiencies were low in particularly for *N,N*-dimethylaminocinnamyl moiety. This could be explained in term of polymer/DNA binding affinity. The chemical structures of MDMBzChC and MDMCMChC were similar but with different chain length between Ch backbone and quaternary ammonium moieties. According to agarose gel electrophoresis (Fig. 4c and d), the MDMCMChC rapidly condensed DNA at N/P ratio 2, whereas the binding of MDMBzChC with DNA was formed later at N/P ratio 2.5. It was postulated that the MDMCMChC would tightly bind to DNA, therefore DNA might not be easily dissociated into cytoplasm, resulting in the lowest gene transfection efficiency. However, the highest gene transfection efficiency was found from MPyMeChC although it contains similar chain length as MDMBzChC. This could be due to better binding affinity of MPyMeChC as compared to the MDMBzChC. The smearing DNA band of MPyMeChC/DNA complex was observed at N/P ratio of 2 (Fig. 4b), whereas free DNA band was found in case of MDMBzChC/DNA complex (Fig. 4c). Therefore, it should be noted that types of quaternary ammonium moiety play an important role for binding affinity. It is known that the structure of DNA comprises of aromatic bases and phosphate groups on the sugar backbone. Therefore, the negative charge of DNA can be neutralized by the positive charge of quaternary ammonium moiety. Moreover, π–π interaction between aromatic bases of DNA and aromatic moieties in the complex might affect the binding affinity. It is possible that positive charge in the pyridine ring could be delocalized by the resonance effect, which would enhance DNA condensation compared to MDMBzChC and TMChC. The difference in transfection efficiency between MPyMeChC and TMChC could be due to the lowest binding affinity of TMChC from gel electrophoresis found at N/P ratio 3.

The substitution of 4-pyridinylmethyl and 4-*N,N*-dimethylaminobenzyl moieties in Ch resulted in enhanced transfection efficiency in Huh7 cells. These results revealed that not only the *N,N,N*-trimethyl groups but also the 4-pyridinylmethyl and 4-*N,N*-dimethylaminobenzyl groups affected the gene transfection efficiency. The MPyMeChC/DNA complex showed the highest transfection efficiency at N/P ratio of 5 then the potential was decreased with increasing N/P ratios. Although at N/P ratio of 40 the transfection efficiency was very low, however, it still had 70% cell viability. Moreover, the transfection efficiency of MPyMeChC/DNA complex was low in HeLa cells compared to Huh7 cells (data not shown). This was due to cellular membrane composition varies among cellular types and many facilitate or hinder the binding of the complexes and subsequent internalization (Corsi, Chellat, Yahia, & Fernandes, 2003). Although the exact mechanism of

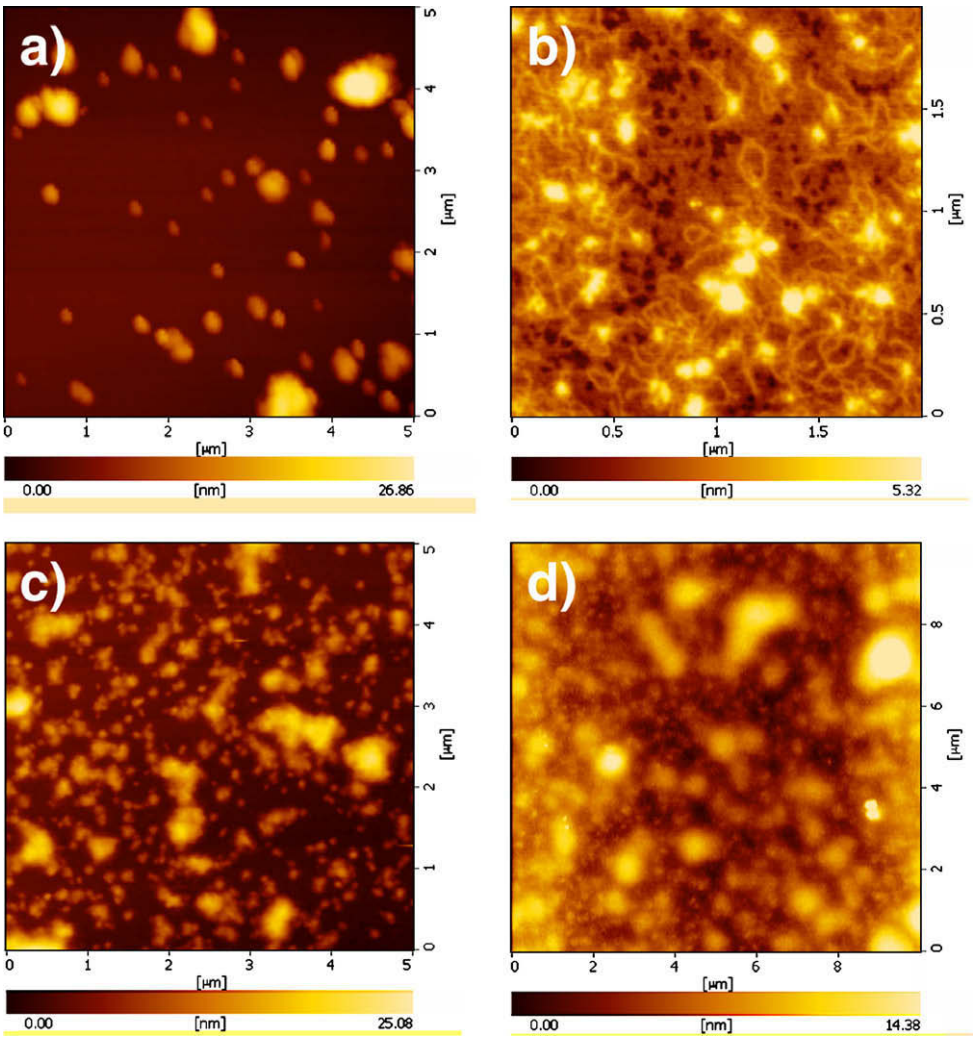

Fig. 6. AFM topography images of DNA complexes with *N*,*N*,*N*-Trimethyl chitosan chloride (TMChC), (b) methylated *N*-(4-pyridinylmethyl) chitosan chloride (MPyMeChC), (c) methylated *N*-(4-*N*,*N*-dimethylaminobenzyl) chitosan chloride (MDMBzChC), and (d) methylated *N*-(4-*N*,*N*-dimethylaminocinnamyl) chitosan chloride (MDMDMChC) at N/P ratios 3, 2.5, 2.5 and 2, respectively.

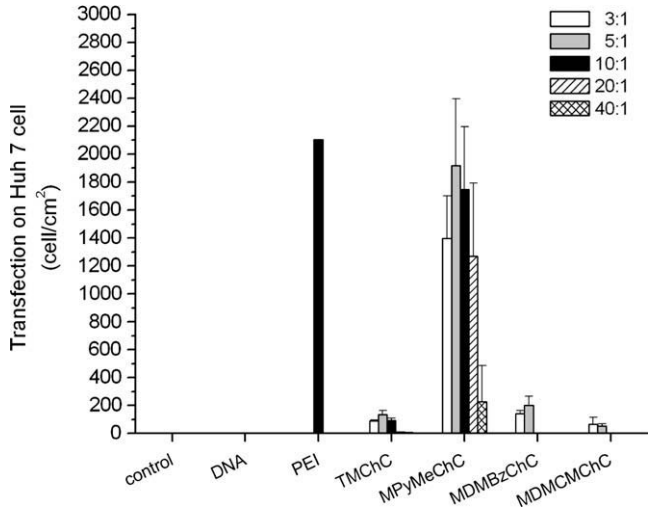

Fig. 7. Transfection efficiencies of methylated chitosan derivatives/DNA complexes in Huh 7 cell lines at various N/P ratios of 3, 5, 10, 20, and 40 compared with polyethylenimine (PEI) DNA complex.

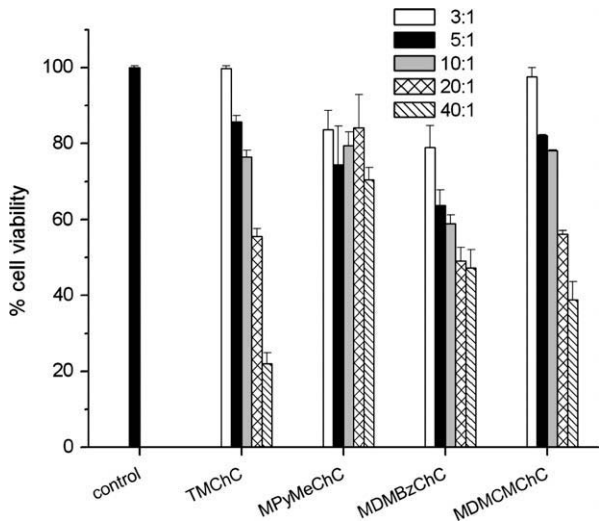

Fig. 8. Cell viability of methylated chitosan derivatives/DNA complexes in Huh 7 cell lines at various N/P ratios of 3, 5, 10, 20, and 40, respectively.

MPyMeChC mediated efficient gene delivery remain to be further studied, our study showed that MPyMeChC could be a potential candidate for non-viral gene carriers.

5. Conclusion

The water-soluble chitosan derivatives, MPyMeChC, MDMBzChC and MDMCMChC, were successfully synthesized. *In vitro* transfection efficiencies of methylated chitosan derivatives/DNA complexes were dependent on N/P ratios and chemical structures of polymers. The MPyMeChC exhibited highest transfection efficiency in Huh 7 cells compared to other methylated chitosan derivatives. The methylated *N*-(4-pyridinylmethyl) chitosan with similar degree of quaternization could increase not only on solubility but also on transfection efficiency. Our study indicated that the chemical structure and the positive charge location play an important role for binding affinity.

Acknowledgements

We gratefully acknowledge the financial support from the Research, Development and Engineering (RD&E) Fund through National Nanotechnology Center (NANOTEC), National Science and Technology Development Agency (NSTDA), Thailand (Project No. NN-B-22-EN4-94-51-10).

References

Allen, M. J., Bradbury, E. M., & Balhorn, R. (1997). AFM analysis of DNA–protamine complexes bound to mica. *Nucleic Acids Research, 25*, 2221–2226.

Anderson, D. G., Akinc, A., Hossain, N., & Langer, R. (2005). Structure/property studies of polymeric gene delivery using a library of poly(β-amino esters). *Molecular Therapy, 11*, 426–434.

Boussif, O., Lezoualc'h, F., Zanta, M. A., Mergny, M. D., Scherman, D., Demeneix, B., et al. (1995). A versatile vector for gene and oligonucleotide transfer into cells in culture and in vivo: Polyethylenimine. *Proceedings of the National Academy of Sciences of the USA, 92*, 7297–7301.

Brugnerotto, J., Lizardi, J., Goycoolea, F. M., Argüelles-Monal, W., Desbrières, J., & Rinaudo, M. (2001). An infrared investigation in relation with chitin and chitosan characterization. *Polymer, 42*, 3569–3580.

Chae, S. Y., Son, S., Lee, M., Jang, M. K., & Nah, J. W. (2005). Deoxycholic acid-conjugated chitosan oligosaccharide nanoparticles for efficient gene carrier. *Journal of Controlled Release, 109*, 330–344.

Check, E. (2005). Gene therapy put on hold as third child develops cancer. *Nature, 433*, 561.

Corsi, K., Chellat, F., Yahia, L., & Fernandes, J. C. (2003). Mesenchymal stem cells, MG63 and HEK293 transfection using chitosan–DNA nanoparticles. *Biomaterials, 24*, 1255–1264.

Crini, G., Torri, G., Guerrini, M., Morcellet, M., Weltrowski, M., & Martel, B. (1997). NMR characterization of *N*-benzyl sulfonated derivatives of chitosan. *Carbohydrate Polymers, 33*, 145–151.

Doody, A. M., Korley, J. N., Dang, K. P., Zawaneh, P. N., & Putnam, D. (2006). Characterizing the structure/function parameter space of hydrocarbon-conjugated branched polyethylenimine for DNA delivery in vitro. *Journal of Controlled Release, 116*, 227–237.

Elisabete, C., Douglas, D. B., & Sergio, P. C. F. (2003). Methylation of chitosan with iodomethane: Effect of reaction conditions on chemoselectivity and degree of substitution. *Macromolecular BioScience, 3*, 571–576.

Germershaus, O., Mao, S., Sitterberg, J., Bakowsky, U., & Kissel, T. (2008). Gene delivery using chitosan, trimethyl chitosan or polyethylenglycol–graft–trimethyl chitosan block copolymers: Establishment of structure–activity relationships in vitro. *Journal of Controlled Release, 125*, 145–154.

Golan, R., Pietrasanta, L. I., Hsieh, W., & Hansma, H. G. (1999). DNA toroids: Stages in condensation. *Biochemistry, 38*, 14069–14076.

Guy, J., Drabek, D., & Antoniou, M. (1995). Delivery of DNA into mammalian cells by receptor-mediated endocytosis and gene therapy. *Molecular Biotechnology, 3*, 237–248.

Hollon, T. (2000). Researchers and regulators reflect on first gene therapy death. *Nature Medicine, 6*, 6–14.

Kean, T., Roth, S., & Thanou, M. (2005). Trimethylated chitosans as non-viral gene delivery vectors: Cytotoxicity and transfection efficiency. *Journal of Controlled Release, 103*, 643–653.

Kim, C. H., Choi, J. W., Chun, H. J., & Choi, K. S. (1997). Synthesis of chitosan derivatives with quaternary ammonium salt and their antibacterial activity. *Polymer Bulletin, 38*, 387–393.

Kim, T. H., Jiang, H. L., Jere, D., Park, I. K., Cho, M. H., Nah, J. W., et al. (2007). Chemical modification of chitosan as a gene carrier in vitro and in vivo. *Progress in Polymer Science, 32*, 726–753.

Kneuer, C., Sameti, M., Bakowsky, U., Schietstel, T., Schirra, H., Schmidt, H., et al. (2000). A nonviral DNA delivery system based on surface modified silica-nanoparticles can efficiently transfect cells in vitro. *Bioconjugate Chemistry, 11*, 926–932.

Köping-Höggård, M., Tubulekas, I., Guan, H., Edwards, K., Nilsson, M., Vårum, K. M., et al. (2001). Chitosan as a nonviral gene delivery system. Structure–property relationships and characteristics compared with polyethylenimine in vitro and after lung administration in vivo. *Gene Therapy, 8*, 1108–1121.

Lavertu, M., Xia, Z., Serreqi, A. N., Berrada, M., Rodrigues, A., Wang, D., et al. (2003). A validated ^{1}H NMR method for the determination of the degree of deacetylation of chitosan. *Journal of Pharmaceutical and Biomedical Analysis, 32*, 1149–1158.

Lee, K. Y., Kwon, I. C., Kim, Y. H., Jo, W. H., & Jeong, S. Y. (1998). Preparation of chitosan self-aggregates as a gene delivery system. *Journal of Controlled Release, 51*, 213–220.

Lv, H., Zhang, S., Wang, B., Cui, S., & Yan, J. (2006). Toxicity of cationic lipids and cationic polymers in gene delivery. *Journal of Controlled Release, 114*, 100–109.

Mansouri, S., Cuie, Y., Winnik, F., Shi, Q., Lavigne, P., Benderdour, M., et al. (2006). Characterization of folate–chitosan–DNA nanoparticles for gene therapy. *Biomaterials, 27*, 2060–2065.

Mansouri, S., Lavigne, P., Corsi, K., Benderdour, M., Beaumont, E., & Fernandes, J. C. (2004). Chitosan–DNA nanoparticles as non-viral vectors in gene therapy: Strategies to improve transfection efficacy. *European Journal of Pharmaceutics and Biopharmaceutics, 57*, 1–8.

Martin, A. L., Davies, M. C., Rackstraw, B. J., Roberts, C. J., Stolnik, S., Tendler, S. J. B., et al. (2000). Observation of DNA–polymer condensate formation in real time at a molecular level. *Federation of European Biochemical Societies Letters, 480*, 106–112.

Merdan, T., Kopeček, J., & Kissel, T. (2002). Prospects for cationic polymers in gene and oligonucleotide therapy against cancer. *Advanced Drug Delivery Reviews, 54*, 715–758.

Murata, J., Ohya, Y., & Ouchi, T. (1997). Design of quaternary chitosan conjugate having antennary galactose residues as a gene delivery tool. *Carbohydrate Polymers, 32*, 105–109.

Nomura, T., Nakajima, S., Kawabata, K., Yamashita, F., Takakura, Y., & Hashita, M. (1997). Intratumoral pharmacokinetics and in-vivo gene expression of naked plasmid DNA and its cationic liposome complexes after direct gene transfer. *Cancer Research, 57*, 2681–2686.

Ogris, M., Steinlein, P., Carotta, S., Brunner, S., & Wagner, E. (2001). DNA/polyethylenimine transfection particles: Influence of ligands, polymer size and PEGylation on internalisation and gene expression. *American Association of Pharmaceutical Scientists, 3*(3), 43–53.

Ogris, M., Steinlein, P., Kursa, M., Mechtler, K., Kircheis, R., & Wagner, E. (1998). The size of DNA/transferrin-PEI complexes is an important factor for gene expression in cultured cells. *Gene Therapy, 5*, 1425–1433.

Putnam, D. (2006). Polymers for gene delivery across length scales. *Natural Materials, 5*, 439–451.

Sajomsang, W., Tantayanon, S., Tangpasuthadol, V., & Daly, W. H. (2008). Synthesis of methylated chitosan containing aromatic moieties: Chemoselectivity and effect on molecular weight. *Carbohydrate Polymers, 72*, 740–750.

Sieval, A. B., Thanou, M., Kotzé, A. F., Verhoef, J. C., Brussee, J., & Junginger, H. E. (1998). Preparation and NMR characterization of highly substituted *N*-trimethyl chitosan chloride. *Carbohydrate Polymers, 36*, 157–165.

Snyman, D., Hamman, J. H., & Kotze, A. F. (2003). Evaluation of the mucoadhesive properties of *N*-trimethyl chitosan chloride. *Drug Development and Industrial Pharmacy, 29*, 61–69.

Thanou, M., Florea, B. I., Geldof, M., Junginger, H. E., & Borchard, G. (2002). Quaternized chitosan oligomers as novel gene delivery vectors in epithelial cell lines. *Biomaterials, 23*, 153–159.

Tian, H., Xiong, W., Wei, J., Wang, Y., Chen, X., Jing, X., et al. (2007). Gene transfection of hyperbranched PEI grafted by hydrophobic amino acid segment PBLG. *Biomaterials, 28*, 2899–2907.

Wagner, E., Kircheis, R., & Walker, G. F. (2004). Targeted nucleic acid delivery into tumors: New avenues for cancer therapy. *Biomedicine and Pharmacotherapy, 58*, 152–161.

Weecharangsan, W., Opanasopit, P., Ngawhirunpat, T., Rojanarata, T., & Apirakaramwong, A. (2006). Chitosan lactate as a nonviral gene delivery vector in COS-1 cells. *American Association of Pharmaceutical Scientists, 7*(3), E74–E79.

Wong, S. Y., Pelet, J. M., & Putman, D. (2007). Polymer systems for gene delivery – Past, present, and future. *Progress in Polymer Science, 32*, 799–837.

Zhang, S., Xu, Y., Wang, B., Qiao, W., Liu, D., & Li, Z. (2004). Cationic compounds used in lipoplexes and polyplexes for gene delivery. *Journal of Controlled Release, 100*, 165–180.